Energy Conversion and Management 175 (2018) 151–163

Contents lists available at ScienceDirect

Energy Conversion and Management

journal homepage: www.elsevier.com/locate/enconman

Particle swarm optimisation with adaptive mutation strategy for photovoltaic solar cell/module parameter extraction

Manel Merchaoui*, Anis Sakly, Mohamed Faouzi Mimouni

Electrical Department, National Engineering School of Sousse, University of Sousse, Tunisia

ARTICLE INFO

Keywords:
PSO
Adaptive mutation
Parameter extraction
Solar modules

ABSTRACT

Developing an accurate model for photovoltaic solar cell and module represents a challenge to improve the overall efficiency of the photovoltaic systems use. Parameter estimation of photovoltaic solar cell and module circuit model is a crucial task that is commonly transformed into an optimisation issue solved by metaheuristic algorithms. Among these algorithms, the particle swarm optimisation has gained great interest due to its structure simplicity and rapid response. However, its major disadvantage lies in the premature convergence. In an endeavour to deal with this problem, an improved mutated particle swarm optimisation algorithm with adaptive mutation strategy is proposed in this paper. The adaptive mutation is introduced to alleviate the premature convergence problem and ensure a suitable trade-off between the explorative and exploitative capabilities over the search process. The proposed algorithm is used to identify the optimal parameters of different photovoltaic models; single diode, double diode, and photovoltaic module. The performance of the used method is firstly evaluated on measured data reported in the literature. Then, the algorithm is tested based on measured data from the laboratory work and from the data sheet of different modules. Experimental results prove that the used algorithm achieves higher accuracy and provides the lowest root mean square error compared to other previously reported parameter extraction algorithms.

1. Introduction

The use of renewable energy, as an alternative to standard fossil-fuel, in electricity generation, is vigorously rising as a way to deal with the energy crisis circumstances. Among the diverse kinds of renewable energy resources, the solar energy is the most used for electricity generation all over the world. In fact, it presents a clean, sustainable, and eco-friendly energy resource to humanity.

The photovoltaic (PV) technology based on the conversion of solar energy to electrical power, has gained the interest of several researchers. In fact, the solar PV is an economic and inexhaustible energy source characterized by an easy maintenance [1]. The efficiency of the PV system is a paramount task to optimally exploit the converted energy. To ameliorate the performance of the PV system, an appropriate model of PV cells and modules is required. PV solar cell modelling consists of mathematically describing its non-linear (I-V) characteristic. In this context, several mathematical models have been provided by the literature. The most popular are based on the single and double diode models [2]. The single diode model (SDM) is commonly used in practice since it ensures the compromise between simplicity and accuracy. The double diode model (DDM) is more accurate, but requires an extensive range of computation. Regardless of the different types of models, the estimation of the PV model's optimal parameters is of crucial significance to design and simulate the optimal PV system behaviour [3].

Considering the great importance of the PV parameter estimation, different approaches have been established in the literature. These approaches have been classified into two common categories; analytical and numerical approaches. The first one is based on the information provided by the manufacturer's data sheet such as short-circuit current (I_{sc}), open circuit-voltage (V_{co}), and maximum power voltage and current (V_{mpp}, I_{mpp}) [4]. As the manufacturer provides information only at Standard Test Condition (STC), this approach remains inappropriate with regard to temperature and irradiation variation. In addition, the analytical methods commonly introduce simplifying assumptions that decrease the model accuracy and lead to improper parameter evaluation [5].

The numerical approach is based on curve fitting through non-linear optimisation algorithms regardless of climatic conditions. These optimisation algorithms may be organised into two categories: conventional or iterative and metaheuristic optimisation methods. To be appropriate for use, the conventional methods, such as Newton-Raphson technique [6] and Levenberg-Marquardt technique [7], require

* Corresponding author.
E-mail address: merchaouimanel@hotmail.fr (M. Merchaoui).

https://doi.org/10.1016/j.enconman.2018.08.081
Received 3 April 2018; Received in revised form 27 June 2018; Accepted 22 August 2018
Available online 05 September 2018

convexity, continuity and differentiability, resulting in a wide range of computation. Moreover, the iterative methods often trap into local optima when the initialisation is far from the optimal parameters, as the reliability of the evaluated model is vigorously sensitive to parameters' initialisation.

Recently, metaheuristic optimisation methods have drawn significant interest toward PV parameter extraction problems to overcome the drawbacks of analytical and iterative techniques. In fact, they are characterised by their global search process to avoid leading to local optimum and their ability to handle non-linear problems without gradient calculation and initialisation constraints. Among the commonly used evolutionary algorithms (EAs): the Genetic Algorithm (GA) [8], the Pattern Search (PS) [9], the Simulated Annealing (SA) [10], the Bird Mating (BM) [11], the Artificial Bee Swarm Optimisation (ABSO) [12], and the Particle Swarm Optimisation (PSO) [13]. In case of the GA, significant shortcomings have been identified including low speed convergence due to enormous calculation effort, and degradation in efficiency for highly interactive fitness function [14]. Regarding the PS algorithm, if the chosen pattern is wrong, the algorithm can easily fall into premature convergence [9]. In case of the SA algorithm, the major issue is the trade-off between cooling schedules and matching temperature [10]. In Ref. [3] a mutative-scale parallel chaos optimisation algorithm is employed for PV model parameter estimation. In Ref. [15], Alam et al. utilised the Flower Pollination Algorithm (FPA) based solar cell and module parameter extraction. In [16] an enhanced variant of FPA was applied in this context. A hybrid algorithm based on FPA and Nelder-Mead simplex method is applied in [17] to improve the accuracy and convergence speed for PV model parameter estimation. Authors in [18], proposed an adaptive differential evolution algorithm to solve PV model parameter extraction. Five different variants of the Bacterial Foraging Algorithm (BFA) were developed, in [19], to identify the PV module parameters from nameplate data. In [20], an improved Jaya algorithm was developed to accurately extract the parameters of PV models. In [21], an imperialist competitive algorithm was used to extract the optimal parameter of the PV model.

The PSO algorithm is widely discussed and used for PV models parameters extraction. In fact, it is characterised by a simple structure, fast response and reduced number of tuning parameters. Ye et al. [22], used the PSO to evaluate the SDM and DDM solar cell parameters. In comparison with GA algorithm, the PSO has shown better performance with regard to the accuracy, complexity and convergence speed. The PSO algorithm is applied in [23] to estimate the parameters of a PV three diode model. However, as other metaheuristic algorithms, the major problem of the PSO lies in the premature convergence, so that the algorithm can converge to a local optimum resulting in a low quality solution. A great deal of effort has already been applied to alleviate the premature convergence of the PSO algorithm. In Ref. [24], the authors added a cluster analysis procedure to the PSO based extracting algorithm. However, this method is bulky enough and consumes more memory and time of computation as it memorises all the previous calculated data. An improved PSO algorithm with a modified inertia weight is applied in [25] for solar cell parameters extraction. In Ref. [26], authors employed Chaos Particle Swarm Optimisation to determine the unknown parameters of the SDM solar cell and module. The chaotic search process is required to reinitiate the particles when they are stagnated to improve the local and global search. To improve the search process, in Ref. [27], the author used a modified variant of PSO, where the acceleration coefficients and the inertia weight are varying with time to ameliorate the exploration and exploitation capabilities of the algorithm. However, this strategy may result in an inappropriate adjustment of the PSO parameters and lead to local convergence. In [28], to avoid possible premature convergence and improve the diversity of the swarm, the PSO algorithm with binary constraints is used to evaluate the diode ideality factor, shunt resistance and series resistance of the single diode model under varying environmental conditions.

The main contribution of this research is to propose an improved mutated PSO (MPSO) with adaptive mutation strategy to solve the PV parameter extraction problem. The main idea of the proposed MPSO is to ameliorate the explorative capability of the PSO algorithm to ensure the convergence to the global optimum. In this context, the mutation is important during the first generations, so that the algorithm may efficiently explore different areas of the search space and locate the region including the global optimum. Over the last generations, the mutation process decreases so that the PSO can perform a better exploitation capability. In this way, a suitable trade- off between the exploration and the exploitation phases of the PSO is achieved resulting in a high quality of the PV solar system modelling.

The remainder of the article is organised as follows. Section 2 briefly discuss PV models. The optimisation problem for PV parameter estimation is formulated in Section 3. Section 4 describes the standard PSO. In Section 5 the proposed mutated PSO is explained. Section 6 will discuss simulation and experimental results and the conclusion is presented in Section 7.

2. Solar photovoltaic modelling

The most commonly used models that illustrate the behaviour and the operation of the PV solar cells are the single and double diode lumped circuit models [16]. In this section, these models are briefly explained.

2.1. Single diode model

Under illumination and normal operating conditions, the single diode model (SDM) is commonly used for PV solar cell modelling. In fact, it guaranties the trade-off between accuracy and simplicity. The equivalent electrical circuit is illustrated in Fig. 1a. It contains an electric current source I_L associated in parallel with a diode, a shunt resistance R_p symbolising the leakage current and a series resistance R_s representing the ohmic losses and the material resistivity. According to this model, the output electric current is given by Eq. (1):

$$I = I_L - I_d - I_p \tag{1}$$

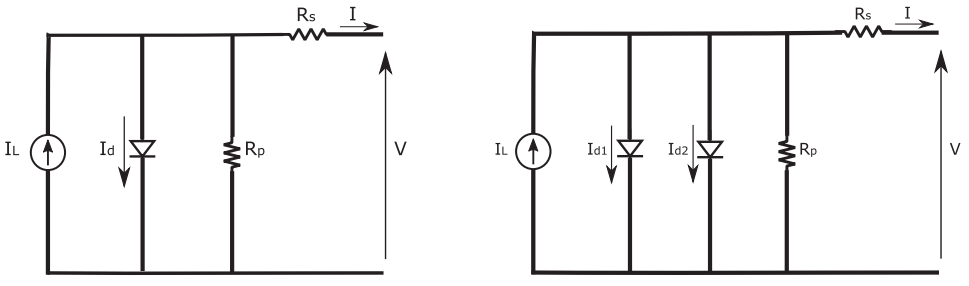

(a) Single Diode Model (SDM) (b) Double diode model (DDM)

Fig. 1. PV solar cell modelling.

Table 1
RMSE and extracted parameters comparison between MPSO and other state-of-the-art algorithms for SDM RTC France silicon solar cell.

Parameters	CPSO [27]	ABSO [12]	PS [9]	SA [10]	GA [32]	DET [18]	MPCOA [3]	TVACPSO [27]	FPA [15]	GOFPANM [17]	MPSO
I_L (A)	0.760788	0.7608	0.7617	0.7620	0.7619	0.751	0.76073	0.760788	0.76079	0.7607755	0.760787
I_s (μA)	0.3106975	0.30623	0.9980	0.4798	0.8087	0.315	0.32655	0.3106827	0.310677	0.3230208	0.310683
R_s (Ω)	0.036547	0.03659	0.0313	0.0345	0.0299	0.036	0.03635	0.036547	0.0365466	0.0363771	0.036546
R_p (Ω)	52.892521	52.2903	64.1026	43.1034	42.3729	54.532	54.6328	52.889644	52.8771	53.7185203	52.88971
n	1.475262	1.47583	1.6000	1.5172	1.5751	1.487	1.48168	1.475258	1.47707	1.4811836	1.475262
RMSE	7.7301e−4	9.9124e−4	0.01494	0.01900	0.01908	9.3e−4	9.4457e−4	7.7301e−4	7.7301e−4	9.8602e−04	7.73006–4

Table 2
RMSE and extracted parameters comparison between MPSO and other state-of-the-art algorithms for DDM RTC France silicon solar cell.

Parameters	CPSO [27]	ABSO [12]	PS [9]	SA [10]	DET [18]	MPCOA [3]	TVACPSO [27]	FPA [15]	GOFPANM [17]	MPSO
I_L (A)	0.760805	0.76078	0.7602	0.7623	0.76098	0.76078	0.760809	0.760795	0.7607811	0.760812
I_{s1} (μA)	0.9575723	0.26713	0.9889	0.4767	0.33267	0.31259	0.004046782	0.300088	0.7493476	0.008971
I_{s2} (μA)	0.334501	0.38191	0.0001	0.01	0.0647	0.04528	0.9274655	0.166159	0.2259743	2.136189
R_s (Ω)	0.037353	0.03657	0.032	0.0345	0.03685	0.03635	0.037973	0.0363342	0.0367404	0.037994
R_p (Ω)	55.441518	54.6219	81.3008	43.1034	54.5321	54.2531	56.549605	52.3475	55.4854485	58.24134
n_1	1.881069	1.46512	1.6	1.5172	1.48735	1.47844	1.327160	1.47477	2	1.373644
n_2	1.407490	1.98152	1.192	2.0000	1.7956	1.78459	1.735315	2.0000	1.4510168	2.0000
RMSE	7.4444e−4	9.8344e−4	1.5180e−2	0.01664	0.000924	9.2163e−4	7.4365e−4	7.8425e−4	9.8248e−04	7.3257e−4

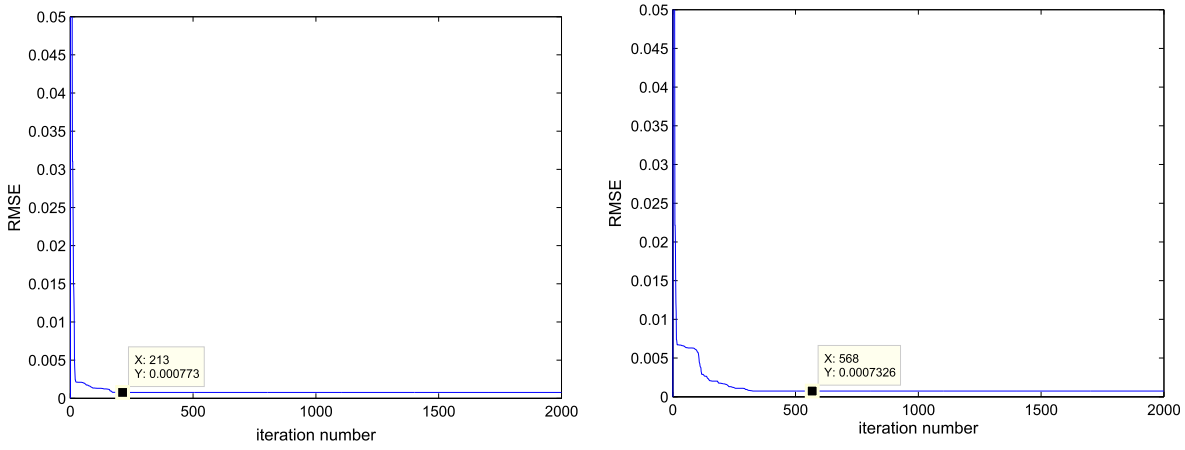

(a) Convergence graph for the SDM (b) Convergence graph for the DDM

Fig. 2. Convergence graphs of the MPSO for RTC France solar cell for the SDM and DDM.

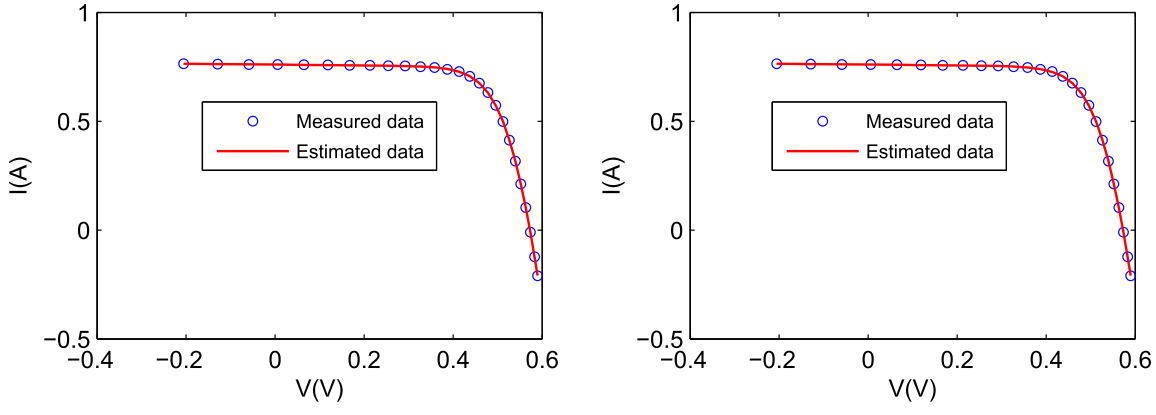

(a) SDM (b) DDM

Fig. 3. Estimated and measured (I-V) characteristics for RTC France solar cell.

Table 3
Individual absolute error and relative error for each measured electric current of RTC France solar cell.

			SDM			DDM		
No.	V_m (V)	I_m (A)	I_{es} (A)	*IAE* (A)	*RE*	I_{es} (A)	*IAE* (A)	*RE*
1	−0.2057	0.7640	0.764149	0.000149	−0.000195	0.763848	0.000151	0.000198
2	−0.1291	0.7620	0.762702	0.000702	−0.000921	0.762533	0.000533	−0.000700
3	−0.0588	0.7605	0.761373	0.000873	−0.001148	0.761326	0.000826	−0.001086
4	0.0057	0.7605	0.760154	0.000345	0.000454	0.760216	0.000283	0.000372
5	0.0646	0.7600	0.759039	0.000960	0.001264	0.759196	0.000803	0.001057
6	0.1185	0.7590	0.758010	0.000989	0.001303	0.758245	0.000754	0.000994
7	0.1678	0.7570	0.757045	4.569546e−5	−6.036388e−05	0.757331	0.000331	−0.000437
8	0.2132	0.7570	0.756084	0.000915	0.001208	0.756381	0.000618	0.000816
9	0.2545	0.7555	0.755022	0.000477	0.000632	0.755278	0.000221	0.000293
10	0.2924	0.7540	0.753597	0.000402	0.000534	0.753748	0.000251	0.000333
11	0.3269	0.7505	0.751327	0.000827	−0.001102	0.751318	0.000818	−0.001090
12	0.3585	0.7465	0.747305	0.000805	−0.001078	0.747109	0.000609	−0.000816
13	0.3873	0.7385	0.740084	0.001584	−0.002145	0.739733	0.001233	−0.001669
14	0.4137	0.7280	0.727426	0.000573	0.000788	0.727017	0.000982	0.001350
15	0.4373	0.7065	0.707025	0.000525	−0.000744	0.706699	0.000199	−0.000282
16	0.4590	0.6755	0.675400	9.966113e−05	0.000147	0.675278	0.000221	0.000327
17	0.4784	0.6320	0.630998	0.001001	0.001585	0.631113	0.000886	0.001403
18	0.4960	0.5730	0.572174	0.000825	0.001440	0.572452	0.000547	0.000955
19	0.5119	0.4990	0.499538	0.000538	−0.001080	0.499837	0.000837	−0.001677
20	0.5265	0.4130	0.413484	0.000484	−0.001174	0.413666	0.000666	−0.001613
21	0.5398	0.3165	0.317161	0.000661	−0.002090	0.317153	0.000653	−0.002063
22	0.5521	0.2120	0.212016	1.672409e−05	−7.888722e−05	0.211830	0.000169	0.000800
23	0.5633	0.1035	0.102636	0.000863	0.008340	0.102364	0.001135	0.010968
24	0.5736	−0.010	−0.009298	0.000701	0.070169	−0.009514	0.000485	0.048513
25	0.5833	−0.123	−0.124361	0.001361	−0.011067	−0.124352	0.001352	−0.010992
26	0.5900	−0.210	−0.209101	0.000898	0.004277	−0.208813	0.001186	0.005650

Table 4
RMSE and extracted parameters comparison between MPSO and other state-of-the-art algorithms for Photo watt-PWP 201 PV module.

Parameters	CPSO [27]	PS [9]	SA [10]	DET [18]	MPCOA [3]	TVACPSO [27]	FPA [15]	GOFPANM [17]	MPSO
I_L (A)	1.031135	1.0313	1.0331	1.0345	1.03188	1.031435	1.032091	1.0305143	1.032230
I_s (μA)	2.730950	3.1756	3.6642	3.31089	3.37370	2.638610	3.047538	3.4822631	2.552134
R_s (Ω)	1.233794	1.2053	1.1989	1.1063	1.20295	1.235611	1.217583	1.2012710	1.238450
R_p (Ω)	861.485735	714.2857	833.3333	815.647	849.6927	821.595146	811.3721	981.9823286	762.9058
n	47.682643	48.2889	48.8211	48.4379	48.50646	47.556652	48.13128	48.6428351	47.47824
RMSE	2.0530e−3	0.0118	0.0027	0.002131	0.002425	2.0530e−3	0.002054673	0.002425	0.002041

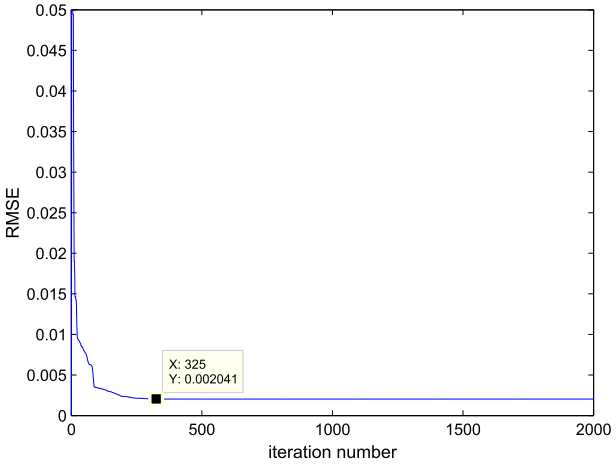

Fig. 4. Convergence graph of the MPSO for Photo watt-PWP 201 PV module.

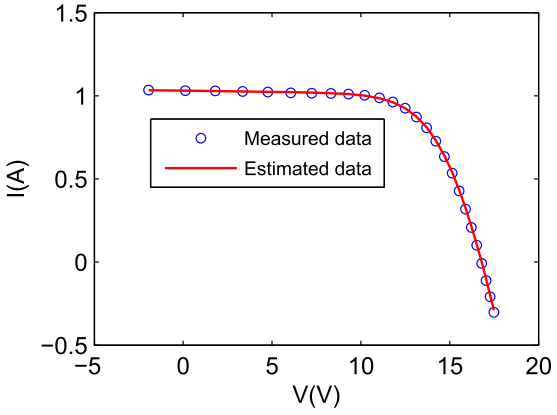

Fig. 5. Estimated and measured (I-V) characteristics for Photo watt-PWP 201 PV module.

where I_L stands for the photogenerated current, I_d represents the diode current and I_p is the current of the shunt resistance. Based on the Shockley equation [29], the diode current is calculated as follows:

$$I_d = I_s\left[\exp\left(\frac{V + IR_s}{nV_T}\right) - 1\right] \quad (2)$$

where I_s represents the reverse saturation current of the diode, n stands for the diode constant, R_s is the series resistance and V_T denotes the thermal voltage given by Eq. (3):

$$V_T = \frac{KT}{q} \quad (3)$$

where $k = 1.3805e^{-13}$ (J/K), is the Boltzmann constant, $q = 1.6e^{-19}$ (C)

Table 5
Individual absolute error and relative error for each measured electric current of the Photo watt-PWP 201 PV module.

No.	V_m (V)	I_m (A)	I_{es} (A)	*IAE* (A)	*RE*
1	−1.9426	1.03450	1.033099	0.001400	0.001354
2	0.1248	1.0315	1.030386	0.001113	0.001079
3	1.8093	1.0300	1.028166	0.001833	0.001779
4	3.3511	1.0260	1.026083	8.394622e−05	−8.18189e−05
5	4.7622	1.0220	1.024064	0.002064	−0.002019
6	6.0538	1.0180	1.021929	0.003929	−0.003860
7	7.2364	1.0155	1.019343	0.003843	−0.003784
8	8.3189	1.0140	1.015681	0.001681	−0.001658
9	9.3097	1.0100	1.009873	0.000126	0.0001253
10	10.2163	1.0035	1.000277	0.003222	0.0032112
11	11.0449	0.9880	0.984616	0.003383	0.0034248
12	11.8018	0.9630	0.960091	0.002908	0.0030201
13	12.4929	0.9255	0.923819	0.001680	0.0018157
14	13.1231	0.8725	0.873551	0.001051	−0.001205
15	13.6983	0.8075	0.808211	0.000711	−0.000880
16	14.2221	0.7265	0.728560	0.002060	−0.002836
17	14.6995	0.6345	0.636630	0.002130	−0.003357
18	15.1346	0.5345	0.535401	0.000901	−0.001686
19	15.5311	0.4275	0.428147	0.000647	−0.001514
20	15.8929	0.3185	0.317774	0.000725	0.0022770
21	16.2229	0.2085	0.206921	0.001578	0.0075703
22	16.5241	0.1010	0.097556	0.003443	0.0340978
23	16.7987	−0.008	−0.00866	0.000667	−0.083493
24	17.0499	−0.111	−0.11102	2.962493e−05	−0.000266
25	17.2793	−0.209	−0.20864	0.000357	0.0017128
26	17.4885	−0.303	−0.30093	0.002067	0.0068221

is the electron charge and T is the cell temperature (°K). The electric current flowing through the shunt resistance R_p is calculated as follows:

$$I_p = \frac{V + IR_s}{R_p} \tag{4}$$

By combining Eqs. (1)–(4), the solar cell current-voltage relationship is given by:

$$I = I_L - I_s\left[\exp\left(\frac{V + IR_s}{nV_T}\right) - 1\right] - \frac{V + IR_s}{R_p} \tag{5}$$

According to Eq. (5), the SDM consists of five unknown parameters to be identified (I_L, I_s, R_s, R_p, n) in order to effectively describe the solar cell behaviour.

2.2. Double diode model

According to the SDM, the effect of the recombination current in the depletion region is neglected. Considering this effect, an additional diode is introduced in the equivalent circuit to achieve an accurate model known as the double diode model (DDM). This model is characterised by a higher accuracy than the SDM. However, it increases the burden of computation.

The equivalent circuit model of a PV cell according to the DDM is depicted in Fig. 1b. The current-voltage relationship is formulated by Eq. (6) [11]:

$$I = I_L - I_{d1} - I_{d2} - \frac{V + IR_s}{R_p} = I_L - I_{s1}\left[\exp\left(\frac{V + IR_s}{n_1 V_T}\right) - 1\right] - I_{s2}\left[\exp\left(\frac{V + IR_s}{n_2 V_T}\right) - 1\right] - \frac{V + IR_s}{R_p} \tag{6}$$

where I_{d1} and I_{d2} denote the electric currents of the first and second diodes, respectively. I_{s1} and I_{s2} represent the reverse saturation currents, n_1 and n_2 are the ideality factors of the two diodes. From Eq. (6), the DDM includes seven unknown parameters to be estimated (I_L, I_{s1}, I_{s2}, R_s, R_p, n_1, n_2).

2.3. Photovoltaic module modelling

Commercial solar modules are composed of a serial connection of numerous cells [18]. Based on the SDM, the current-voltage relationship of a PV module consisting of N_s cells connected in series is described by Eq. (7):

$$I = I_L - I_d - \frac{V + IR_s}{R_p} = I_L - I_s\left[\exp\left(\frac{V + IR_s}{nN_s V_T}\right) - 1\right] - \frac{V + IR_s}{R_p} \tag{7}$$

3. Problem formulation

PV cell and module modelling is based on the extraction of the global optimal parameters of the SDM or DDM based equivalent circuit. The extraction task aims to fit the estimated model with the measured (I-V) data, at any environmental condition, in order to estimate the PV model's optimal parameters. The main target is to minimise the difference between the experimental and estimated data. In this work, the following steps describe the optimisation strategy:

- Measurement of (I-V) data of the PV cell or module curve.
- Definition of the fitness function aiming to reduce the difference between the real and calculated data.
- Tuning the estimated parameters via the optimisation algorithm, in the range of a defined bound, until the stopping criterion is attained.
- Extraction of the model's optimal parameters.

The fitness function is defined so that the calculated parameters minimise the error between the measured and estimated data. In this work, the Root Mean Square Error (RMSE) is used to set the objective function. The RMSE is given by Eq. (8) as in [30]:

$$RMSE = \sqrt{\frac{1}{M}\sum_{j=1}^{M} f(V_m, I_m, X)^2} \tag{8}$$

In the above RMSE, $f(V_m, I_m, X)$ stands for the error function, corresponding to the error between real and calculated data and M is the number of measurements. V_m and I_m are, respectively, the measured voltage and current; X stands for the parameters to be estimated: for the SDM, $X = (I_L, I_s, R_s, R_p, n)$ and for the DDM, $X = (I_L, I_{s1}, I_{s2}, R_s, R_p, n_1, n_2)$. Based on the SDM, the error function is expressed by Eq. (9) [30]:

Table 6
Estimated parameters for IFRI250-60 module at different environmental conditions.

Parameters	(313 W/m²;22.52 °C)	(707.12 W/m²;24.43 °C)	(732.96 W/m²;28.53 °C)	(989.31 W/m²;28.24 °C)
I_L (A)	3.535747	6.285508	6.454701	8.556118
I_s (μA)	3.664293e−4	4.3874350e−2	0.158011	0.589962
R_s (Ω)	1.042582	0.8972312	0.889242	0.861635
R_p (Ω)	911.4892	1399.8134	1408.1877	1426.7622
n	1.005986	1.202399	1.204804	1.252417
RMSE	0.0025999	0.0022226	0.0073067	0.0075589

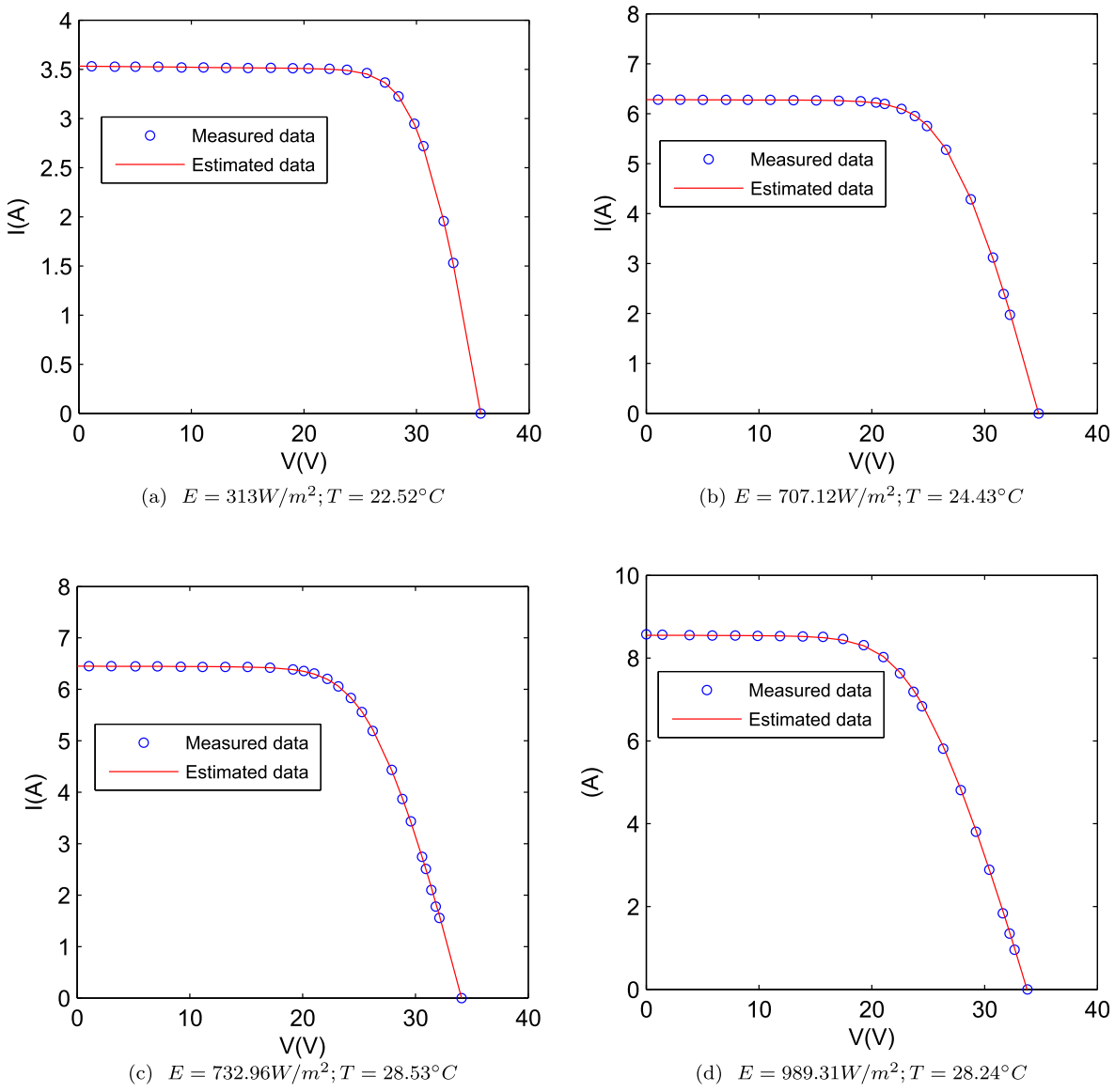

(a) $E = 313W/m^2; T = 22.52°C$ (b) $E = 707.12W/m^2; T = 24.43°C$

(c) $E = 732.96W/m^2; T = 28.53°C$ (d) $E = 989.31W/m^2; T = 28.24°C$

Fig. 6. Estimated and measured (I-V) characteristics for IFRI250-60 module at different environmental conditions.

$$f(V_m, I_m, X) = I_m - I_L + I_s\left[\exp\left(\frac{V_m + I_m R_s}{nV_T}\right) - 1\right] + \frac{V_m + I_m R_s}{R_p} \tag{9}$$

The error function of the DDM is represented by Eq. (10) [30]:

$$f(V_m, I_m, X) = I_m - I_L + I_{s1}\left[\exp\left(\frac{V_m + I_m R_s}{n_1 V_T}\right) - 1\right] + I_{s2}\left[\exp\left(\frac{V_m + I_m R_s}{n_2 V_T}\right) - 1\right] + \frac{V_m + I_m R_s}{R_p} \tag{10}$$

The proposed PSO based optimisation technique is used to minimise the defined objective function (RMSE) to extract the global optimal parameters for the SDM and DDM.

4. Particle swarm optimisation

PSO is a stochastic optimisation algorithm influenced by the collective attitude of animals like fish schooling or bird flocking when they are searching for food. The PSO consists of a group of individuals known as particles. Each particle, considered as a candidate solution, moves in the search area to look for the optimal solution. At the outset, particles are randomly dispersed in the search space. Then, during the search process, each one tunes its position based on its current velocity, its previous best position (P_{best}), and the global best position (G_{best}) of the entire swarm. (P_{best}) and (G_{best}) are crucial to adjust the search direction of the swarm to prevent particles from flying in the same area. At each iteration k, the velocities and positions of the particles are actualised according to the following equations:

$$v_{jd}^{k+1} = \omega v_{jd}^{k} + c_1 r_1 (P_{bestjd} - p_{jd}^{k}) + c_2 r_2 (G_{bestd} - p_{jd}^{k}) \tag{11}$$

$$p_{jd}^{k+1} = p_{jd}^{k} + v_{jd}^{k+1} \tag{12}$$

where v_{jd}^{k} and p_{jd}^{k} denote, respectively, the velocity and the position of the jth particle with respect to the dimension d, ω represents the inertia weight, c_1 and c_2 stand for the cognitive and the social weights, respectively. r_1 and r_2 are random numbers within the range of [0,1]. The principle steps of the standard PSO can be described as follows:

- Step 1: PSO initialisation: particles are initialised with random positions and velocities according to the search range.
- Step 2: Evaluation of the fitness function of each particle.
- Step 3: Memory updating: update the individual best and global best

Table 7
Estimated optimal parameters using MPSO for three types of PV modules at different irradiance and temperature of 25 °C (SDM).

Parameters	Mono-crystalline SM55	Thin-film ST40	Multi-crystalline KC200GT
G = 1000 W/m^2			
I_L (A)	3.4501841	2.67588871	8.2170821
I_s (μA)	0.1670939	1.5005148	2.14017e−3
R_s (Ω)	0.3301288	1.1148351	0.3448508
R_p (Ω)	480.83060	356.134233	753.21483
n	1.3918872	1.4963375	1.0727496
RMSE	0.0010291	5.63979e−4	0.0014250
G = 800 W/m^2			
I_L (A)	2.7604353	2.13807567	6.57165806
I_s (μA)	0.1406415	1.13808651	9.88517e−4
R_s (Ω)	0.3391011	1.12707528	0.35641972
R_p (Ω)	458.11296	332.005139	737.275744
n	1.3774070	1.46939972	1.03555438
RMSE	5.89490e−4	5.92293e−4	0.0014598
G = 600 W/m^2			
I_L (A)	2,07096086	1.60485499	4.93436061
I_s (μA)	0.15060756	1.41766358	3.79720e−3
R_s (Ω)	0.33295359	1.11530132	0.33781806
R_p (Ω)	447.963170	346.988989	739.969017
n	1.38298370	1.49201813	1.10220204
RMSE	7.39595e−4	5.84674e−4	0.0012763
G = 400 W/m^2			
I_L (A)	1.38283252	1.06764748	3.28790536
I_s (μA)	0.10143247	1.75977553	1.43766e−3
R_s (Ω)	0.39516902	1.09107093	0.35531367
R_p (Ω)	427.322060	360.631852	748.820527
n	1.35095066	1.51679224	1.05189287
RMSE	7.04746e−4	5.61749e−4	0.0013888
G = 200 W/m^2			
I_L (A)	0.69150954	0.53293974	1.64614246
I_s (μA)	0.14645817	1,59944136	5.29635e−4
R_s (Ω)	0.28652263	1.13246996	0.37942280
R_p (Ω)	448.217518	347.939096	690.649129
n	1.37881408	1.50848405	1.00261873
RMSE	3.19854e−4	4.682546e−4	0.00141259

Table 8
Estimated optimal parameters using MPSO for three types of PV modules at different irradiance and temperature of 25 °C (DDM).

Parameters	Mono-crystalline SM55	Thin-film ST40	Multi-crystalline KC200GT
G = 1000 W/m^2			
I_L (A)	3.45010996	2.67536366	8.21687557
I_{s1} (μA)	0.15466162	1.31538701	2.20868e−3
I_{s2} (μA)	5.22379979	72.0756959	0.97647996
R_s (Ω)	0.33198742	1.12035080	0.34406217
R_p (Ω)	486.827430	374.226124	763.737199
$n1$	1.38571449	1.48331516	1.07423145
$n2$	3.19765714	4	3.847903729
RMSE	0.0010723	5.94090e−4	0.0014159
G = 800 W/m^2			
I_L (A)	2.76045949	2.13781476	6.57088561
I_{s1} (μA)	0.13816257	1.05975295	9.23968e−4
I_{s2} (μA)	0.32408879	37.4309898	0.30806574
R_s (Ω)	0.33990075	1.13025634	0.35694309
R_p (Ω)	457.644961	340.006212	772.122737
$n1$	1.37598844	1.46247614	1.0325940
$n2$	2.97923915	4	2.13644580
RMSE	5.91087e−4	6.06269e−4	0.0014507
G = 600 W/m^2			
I_L (A)	2.07096416	1.60476606	4.93434901
I_{s1} (μA)	0.14930683	1.35894543	3.80787e−3
I_{s2} (μA)	5.90508801e−2	19.1616733	0.11033868
R_s (Ω)	0.33354314	1.11767283	0.33771723
R_p (Ω)	447.698464	350.547114	740.793539
$n1$	1.38226512	1.48769196	1.10179306
$n2$	3.12677430	4	4
RMSE	7.39755e−4	5.85460e−4	0.0012752
G = 400 W/m^2			
I_L (A)	1.38261937	1.06756191	3.28785611
I_{s1} (μA)	0.11810863	1.72121893	1.41300e−3
I_{s2} (μA)	0.22867046	11.1321812	2.48452480
R_s (Ω)	0.37295640	1.09285459	0.35580832
R_p (Ω)	434.540040	363.446109	752.826434
$n1$	1.36334419	1.51440843	1.05106028
$n2$	2.42288737	4	3.99999987
RMSE	7.32080e−4	5.63589e−4	0.001394076
G = 200 W/m^2			
I_L (A)	0.69159960	0.53288075	1.64600002
I_{s1} (μA)	3.54201e−2	5.72619861	5.12007e−4
I_{s2} (μA)	0.42512140	1.50693146	2.95207170
R_s (Ω)	0.38118569	1.14652335	0.37900827
R_p (Ω)	451.373667	349.578481	701.124377
$n1$	1.27837074	1.50173489	1.00110787
$n2$	1.67758379	3.40485612	3.22359469
RMSE	3.32498e−4	4.65374e−4	0.0014052

fitness values and their positions (P_{bestjd} and G_{bestd}).

- Step 4: Velocity and position updating: The velocity and position of each candidate solution are updated according to Eqs. (11) and (12).
- Step 5: Examination of the convergence criterion: if the convergence criterion is reached, the algorithm can be stopped and outputs the G_{best} as its solution; otherwise, the process will go to step 2.

5. Proposed mutated particle swarm optimisation

Despite the different benefits of metaheuristic optimisation algorithms including the PSO, their major shortcoming is the premature convergence due to the lack of diversity and the deficiency of the exploration phase. In an effort to ameliorate the optimisation process of the PSO, it is crucial to intensify the diversity of the swarm during the first generations and to improve the trade-off between the exploration and exploitation stages. In evolutionary optimisation techniques, such as GA and evolutionary programming, the mutation mechanism is considered to tackle the untimely convergence, and orientate the search process toward the global optimal solution. In this work, to improve the efficiency of the PSO algorithm for solving the PV model parameter extraction problem, the mutation process has been introduced to avoid particles from trapping in local optima. Moreover, to ensure the compromise among the two stages of exploration and exploitation, the mutation mechanism is characterised by an adaptive behaviour. In fact, the mutation process depends on the progress of iterations. Hence, it is important in early generations to help particles to better explore the search space and enhance the diversity of the swarm. Consequently, the particles have a better capability to look for the global optimum in different regions of the search space resulting in high quality solutions. Then, according to the iteration progress, this phenomenon decreases so that the PSO can eventually performs a better exploitation during the last generations.

During the optimisation process, the mutation probability depends on the current iteration. In fact, at each iteration, the mutation probability is calculated, then, for each particle, a random mutation step size is applied to the velocity components that verifying the mutation probability. The mutation step size is given proportionally to the maximum limit of the velocity. The pseudo-code of the proposed mutation process is given by Algorithm 1 MPSO, that is described by the following steps:

- Step 1: Evaluation of the mutation probability.
- Step 2: For each particle, evaluate the fitness function and update

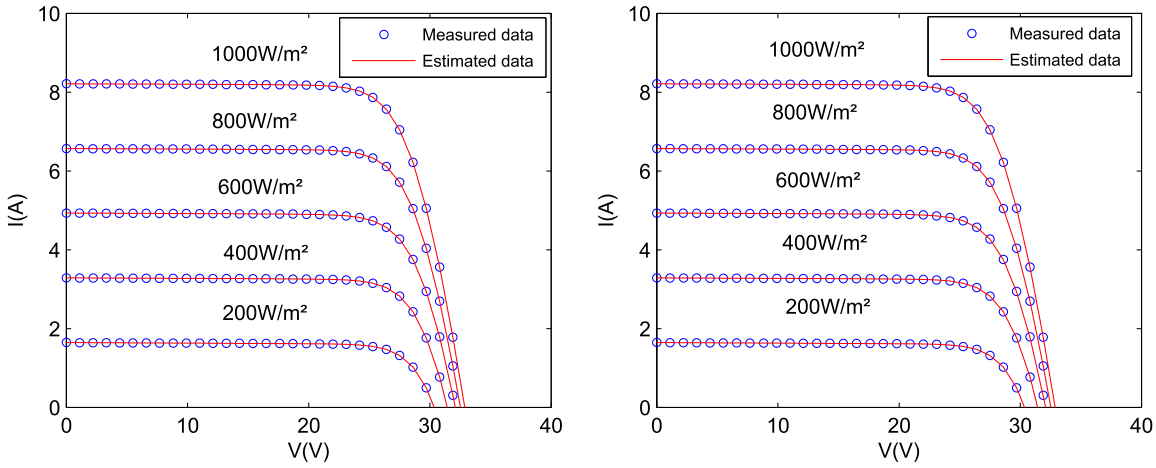

Fig. 7. Estimated and measured (I-V) characteristics for Multi-crystalline KC200GT at different irradiance for both SDM and DDM.

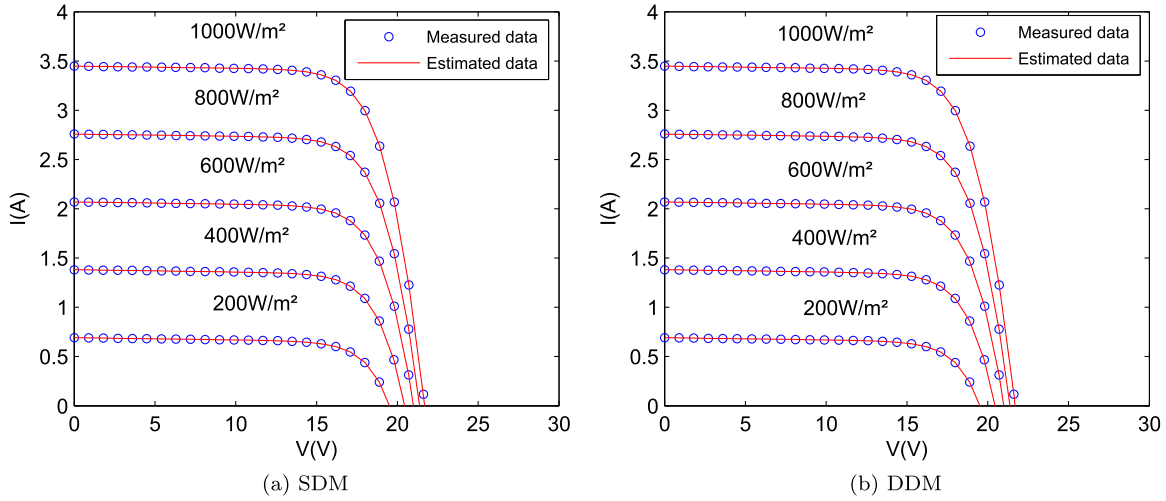

Fig. 8. Estimated and measured (I-V) characteristics for Mono-crystalline SM55 at different irradiance for both SDM and DDM.

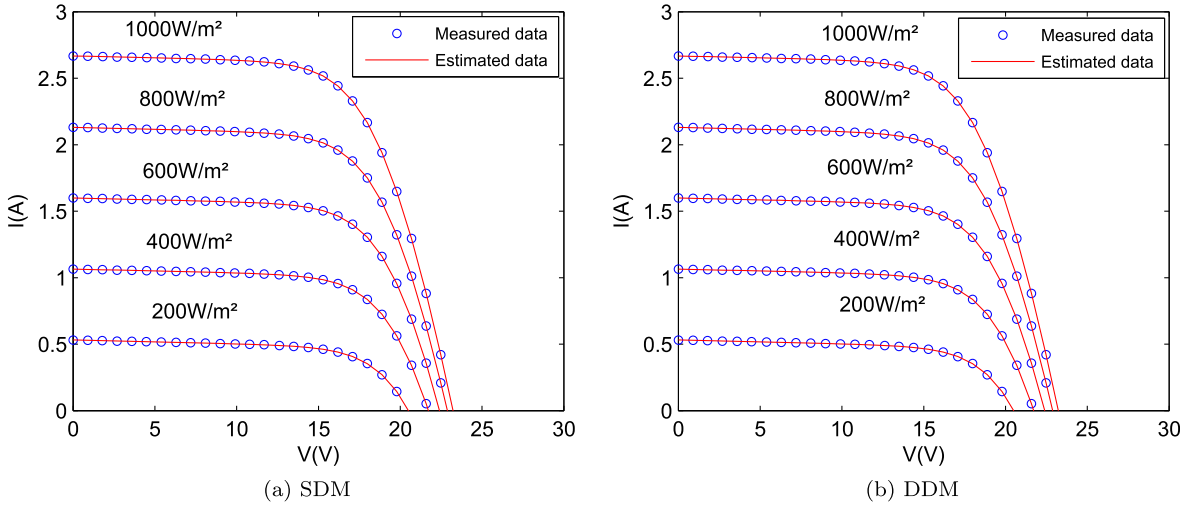

Fig. 9. Estimated and measured (I-V) characteristics for Thin-film ST40 at different irradiance for both SDM and DDM.

Table 9
The optimal extracted parameters for Multi-crystalline KC200GT PV module using the MPSO at different temperatures and irradiance of 1000 W/m^2 (SDM).

Parameters	Temperature		
	(25 °C)	(50 °C)	(75 °C)
SDM			
I_L (A)	8.217082	8.295278	8.378414
I_s (μA)	2.1401e−03	0.125683	1.549389
R_s (Ω)	0.344850	0.344850	0.343649
R_p (Ω)	753.2148	956.2051	736.0917
n	1.072749	1.115647	1.096383
RMSE	0.001425	0.002170	0.002397
DDM			
I_L (A)	8.216875	8.295187	8.377073
I_{s1} (μA)	2.2086e−03	0.125692	1.222878
I_{s2} (μA)	0.976479	5.229062	13.01858
R_s (Ω)	0.344062	0.335716	0.345712
R_p (Ω)	763.7371	968.4855	872.8550
$n1$	1.074231	1.115654	1.081095
$n2$	3.847903	4	1.820552
RMSE	0.001415	0.002175	0.002399

Table 10
The optimal extracted parameters for Mono-crystalline SM55 PV module using the MPSO at different temperatures and irradiance of 1000 W/m^2 (SDM).

Parameters	Temperature		
	(25 °C)	(40 °C)	(60 °C)
SDM			
I_L (A)	3.450184	3.471525	3.495870
I_s (μA)	0.167093	0.569258	5.394662
R_s (Ω)	0.330128	0.356175	0.334735
R_p (Ω)	480.8306	437.4307	431.5450
n	1.391887	1.354581	1.377951
RMSE	0.001029	9.2448e−4	5.1130e−4
DDM			
I_L (A)	3.450109	3.470820	3.495580
I_{s1} (μA)	0.154661	0.388745	4.876215
I_{s2} (μA)	5.223799	31.66379	20.94642
R_s (Ω)	0.331987	0.365691	0.336930
R_p (Ω)	486.8274	482.9742	449.9117
$n1$	1.385714	1.323751	1.368321
$n2$	3.197657	2.825773	2.599879
RMSE	0.001072	8.3629e−4	4.7672e−4

the personal best and the global best.

- Step 3: For each particle, checking the velocity dimensions that will be mutated and applying the mutation process.
- Step 4: Updating the velocity dimensions not verifying the mutation probability based on Eq. (11).
- Step 5: Updating particles positions according to Eq. (12).
- Step 6: Examination of the end criterion.

Algorithm 1. MPSO

while termination condition = false **do**
1 Evaluate the mutation probability = *Pm*;
2 **for** $j = 1$ to number of particles **do**
Evaluate the fitness = $f(x)$;
Update P_{best} and G_{best};
3 **for** $d = 1$ to number of dimensions **do**
if $rand1(1) < P_m$ **then**
if $rand2(1) < 0.5$ **then**
$\upsilon_{jd}^{k+1} = \upsilon_{jd}^{k} + rand(1)\upsilon_{max\_limit}/ms$;
else
$\upsilon_{jd}^{k+1} = \upsilon_{jd}^{k} - rand(1)\upsilon_{max\_limit}/ms$;
end
else
4 $\upsilon_{jd}^{k+1} = \omega\upsilon_{jd}^{k} + c_1 r_1(P_{bestjd} - p_{jd}^{k}) + c_2 r_2(G_{best} - p_{jd}^{k})$;
end
5 $p_{jd}^{k+1} = p_{jd}^{k} + \upsilon_{jd}^{k+1}$;
end
end
end

Table 11
The optimal extracted parameters for Thin-film ST40 PV module using the MPSO at different temperatures and irradiance of 1000 W/m^2 (SDM).

Parameters	Temperature			
	(25 °C)	(40 °C)	(55 °C)	(70 °C)
SDM				
I_L (A)	2.675888	2.681147	2.691130	2.692802
I_s (μA)	1.500514	5.486274	20.68269	84.06207
R_s (Ω)	1.114835	1.131889	1.139613	1.129909
R_p (Ω)	356.1342	359.6524	306.9901	356.2416
n	1.496337	1.470890	1.460075	1.472899
RMSE	5.6397e−4	7.8184e−4	9.6506e−4	5.3900e−4
DDM				
I_L (A)	2.675363	2.680990	2.690905	2.692498
I_{s1} (μA)	1.315387	5.403676	19.30701	58.11806
I_{s2} (μA)	72.07569	24.07619	33.08640	46.79221
R_s (Ω)	1.120350	1.132377	1.142188	1.134734
R_p (Ω)	374.2261	364.6536	314.1012	368.6255
$n1$	1.483315	1.469282	1.452289	1.437114
$n2$	4	4	2.771959	1.754276
RMSE	5.9409e−4	7.8591e−4	9.52564e−4	5.5541e−4

Where $rand(1)$, $rand1(1)$ and $rand2(1)$ are random numbers in the range of $[0, 1]$, ms is a constant corresponding to the mutation step size, υ_{max_limit} represents the maximum velocity, and P_m denotes the adaptive mutation probability defined by the following equation:

$$P_m = a \times \exp\left[\frac{-(k+b)}{c}\right] \tag{13}$$

where k denotes the current iteration number, a and b are constant chosen as follows:

$$\begin{cases} P_m(0) = 1 \\ P_m(max\_iter) = 0.05 \end{cases} \tag{14}$$

where max_iter stands for the maximum iteration number. The mutation probability follows a non-linear exponential variation depending on the current iteration, and it decreases with the progress of iterations. The more the mutation probability is, the more is the diversity of the swarm. Consequently, the more is the exploration capability. During the last generation, the less is the mutation probability, the less is the exploration capability, therefore, the more is the exploitation capability.

6. Simulation and experimental results

The proposed MPSO is validated by extracting the PV optimal parameters, for both SDM and DDM, based on several sources of data, including a commercial silicon solar cell (RTC France), a polycrystalline silicon PV module (Photo Watt-PWP 201), measured data at the laboratory using a multi-crystalline PV module (IFRI250-60), and

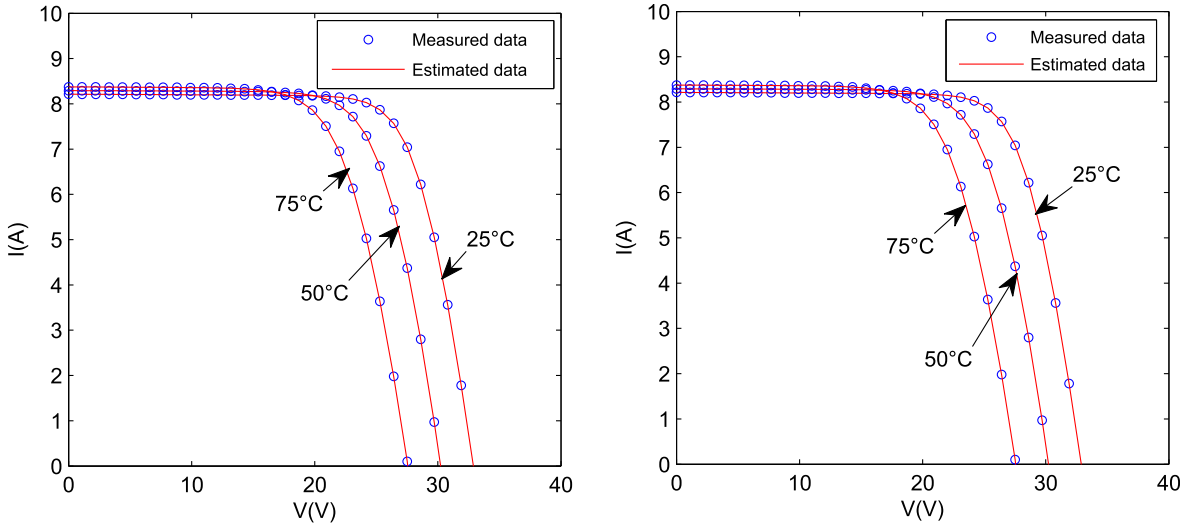

Fig. 10. Estimated and measured (I-V) characteristics for Multi-crystalline KC200GT at different temperatures for SDM and DDM.

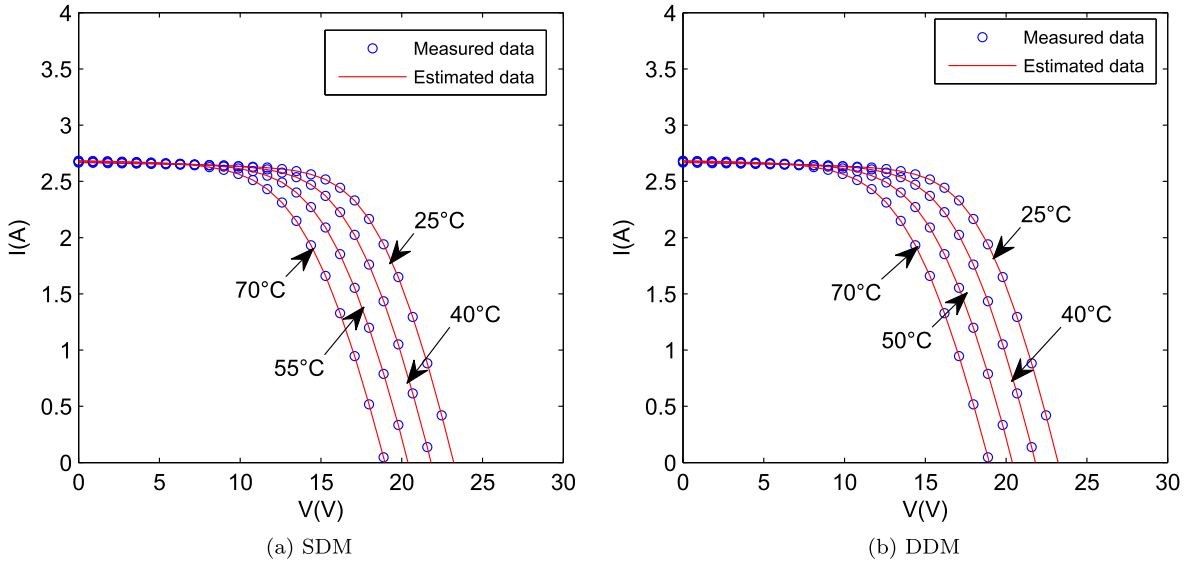

Fig. 11. Estimated and measured (I-V) characteristics for Thin-film ST40 at different temperatures for SDM and DDM.

experimental data from several manufacturer's data sheet. The estimated results are reported and examined. For the MPSO, the inertia weight and the acceleration coefficients are chosen as $\omega = 0.4$, $c_1 = c_2 = 2$, respectively. These parameters were determined by trial and error method through simulations [31]. The maximum number of iterations is set to $max\_iter = 2000$ and represents the stopping criterion for the MPSO. The population size is fixed to 60 particles.

6.1. Results for photovoltaic cells

The measured (I-V) data from a 57 mm diameter commercial (RTC France) silicon solar cell are adopted for parameter evaluation based on both SDM and DDM. The measurements are obtained at an irradiation and a temperature of (1000 W/m^2) and (33 °C), respectively. The measurements include 26 pairs of (I-V) as given in [6]. The bounds of the parameters search range for both SDM and DDM are the same used in [17]. The optimal estimated parameters of the RTC France solar cell are given in Tables 1 and 2 for both SDM and DDM, respectively. The performance of the used algorithm is discussed by comparing the obtained results with others obtained from recent research works, such as Conventional Particle Swarm Optimisation (CPSO) [27], Artificial Bee Swarm optimisation Algorithm (ABSO) [12], Pattern Search (PS) [9], Simulated Annealing (SA) [10], Genetic Algorithm [32], Differential Evolution [18], Mutative-scale Parallel Chaos Optimisation Algorithm (MPCOA) [3], Time varying Acceleration Coefficient Particle Swarm Optimisation (TVACPSO) [27], Flower Pollination Algorithm (FPA) [15], and a hybrid Flower Pollination Algorithm (GOFPANM) [17]. From Table 1, it is noticed that, for the SDM, the proposed technique provides a very low RMSE value that is in agreement with that of CPSO, TVACPSO and FPA and outperforms ABSO, PS, SA, DET, MPCOA and GOFPANM. From Table 2, in the case of DDM, the MPSO outperforms CPSO, TVACPSO, FPA ABSO, PS, SA, DET, MPCOA and GOFPANM as it provides the lowest RMSE value. The convergence graphs of the MPSO have been depicted in Fig. 2, for both SDM and DDM for RTC France solar cell. It is shown that convergence process of the MPSO algorithm reaches the optimal RMSE value equal to 7.73006e−4 at only 213 iterations for the SDM. Moreover, for the DDM, the MPSO achieves the optimal model parameters after 568 iterations at RMSE value equal to 7.3257e−4.

To further evaluate the reliability of the MPSO, the curve fitting is

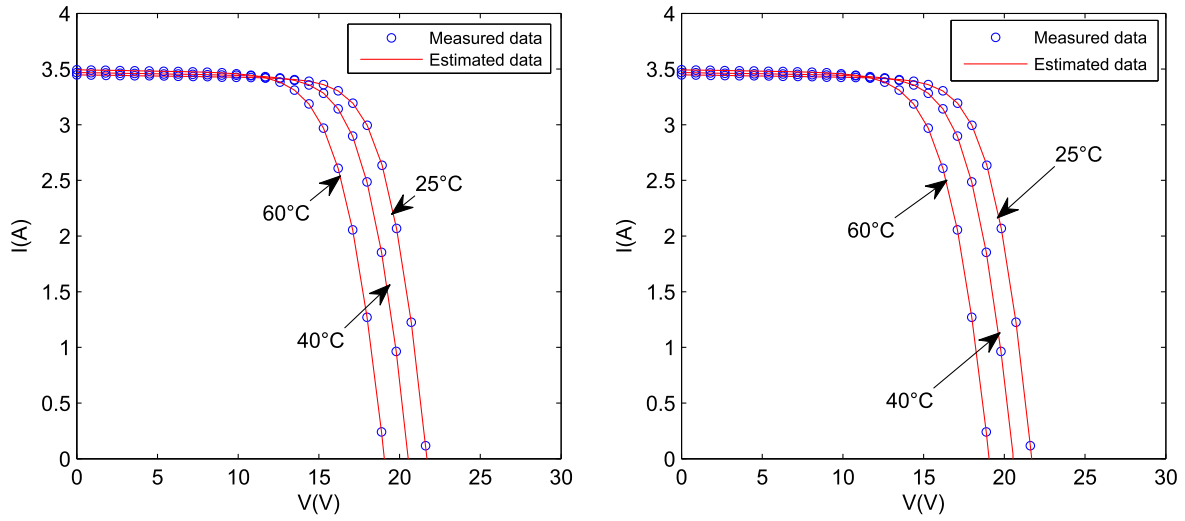

Fig. 12. Estimated and measured (I-V) characteristics for Mono-crystalline SM55 at different temperatures for SDM and DDM.

Table 12
Comparison of MPP data between MPSO algorithm and data sheet under G = 1000 W/m^2 and T = (25 °C).

PV module	Vmpp (V)		Impp (A)		Pmpp (W)		
	Data sheet	MPSO	Data sheet	MPSO	Data sheet	MPSO	Error(%)
SM55	17.4	17.1091	3.15	3.1937	55	54.64	0.65
ST40	16.6	17.0886	2.41	2.33	40	39.81	0.47
KC200GT	26.3	26.4095	7.61	7.57022	200	199.92	0.04

accomplished between calculated and synthetic (I-V) measurements as illustrated in Fig. 3 and it is shown that the estimated and the real data are accurately fitted and ensure a good agreement. Moreover, both of the individual absolute error (IAE) and the relative error (RE) are used to evaluate the error among the measured and estimated data. These two indexes are respectively defined by Eqs. (15) and (16):

$$IAE = |I_m - I_{es}| \tag{15}$$

$$RE = \frac{I_m - I_{es}}{I_m} \tag{16}$$

Table 3, providing the IAE and the RE, proves that the calculated data from the estimated optimal parameters of MPSO are consistent with the experimental data. The IAE values are less than 1.58E−3 for the SDM and less than 1.35E−3 for the DDM. The RE values are within the range of [−1.1E−2, 7E−2] for the SDM and [−1.09E−2, 4.8E−2] for the DDM.

6.2. Results for photovoltaic module

The measured (I-V) data from the Photo Watt-PWP 201 PV module are used for parameter evaluation. The module comprises a series connection of 36 polycrystalline silicon cells. The (I-V) characteristic is measured at an irradiation level of (1000 W/m^2) and a temperature degree of (45 °C) and it consists of 25 pairs of (I-V) values as given in [6]. The bounds of the parameters search range are the same used in [17]. Based on the SDM, the optimal parameters extracted using the MPSO are compared with other techniques like CPSO [27], PS [9], SA [10], DET [18], MPCOA [3], TVACPSO [27], FPA [15], and a hybrid Flower Pollination Algorithm (GOFPANM) [17]. The results are tabulated as Table 4.

The convergence graph of the proposed MPSO algorithm has been plotted in Fig. 4 for Photo watt-PWP 201 PV module. It is shown that the MPSO converges to the optimal result at RMSE value equal to 0.002041 at only 325 iterations. The calculated (I-V) curve using the optimal estimated parameters along with the experimental one validates the accuracy of the estimated optimal parameters, as illustrated in Fig. 5. Accordingly, an appropriate agreement between these two characteristics is ensured. Table 4 proves that the proposed MPSO outperforms the other optimisation algorithms as it reveals the best RMSE value. The IAE and RE are provided in Table 5. The IAE values are less than 3.9E−3 and the RE values are in the range of [−8.3E−2, 3.4E−2], which affirm the agreement of the experimental and estimated electric current data. Consequently, the MPSO represents an appropriate technique to be used for PV module parameter extraction.

6.3. Results for the proposed algorithm with laboratory measurements

The suggested variant of PSO is applied to estimate the optimal parameters for the IFRI250-60 module. It consists of 60 multi-crystalline solar cells connected in series. The electrical parameters given by the manufacturer's data sheet at (*STC*) are given as follows [33]:

- Maximum Power Point *MPP*: 250 W
- Maximum Power voltage V_{MPP}: 31.38 V
- Maximum Power current I_{MPP}: 7.35 A
- Open circuit voltage V_{co} : 37.56 V
- Short circuit current I_{sc}: 8.5 A
- Temperature coefficient of short circuit current: 0.077 (A/°C)
- Temperature coefficient of open circuit voltage: −0.368 (V/°C)

Based on the SDM, the MPSO is used to extract the optimal parameters for IFRI250-60 module using the experimental data recorded at different environmental conditions as given in Table 6. To check the accuracy of the results, the curve fitting between experimental and estimated (I-V) data is elaborated as depicted in Fig. 6. The obtained results prove that the calculated data through the estimated optimal parameters are very close to the experimental data for the whole range of the voltage. Moreover, it is remarkable that, at all environmental conditions, a low RMSE is obtained even under low irradiation level.

6.4. Tests for the proposed method with experimental data from the manufacturer's data sheet

In this section, the reliability of the MPSO, for both SDM and

DDM, is further checked using experimental data from the manufacturer's data sheet of three different PV modules: Mono-crystalline (SM55) [34], Multi-crystalline (KC200GT) [35] and Thin-film (ST40) [36]. The used experimental data are directly extracted from the data sheet at different levels of temperature and irradiation. The search range of the unknown parameters are given as $I_s \in [0, 100]$ (μA), $I_L \in [0, 2I_{sc}]$ (A), $R_s \in [0, 2]$ (Ω), $R_p \in [0, 5000]$ (Ω) and $n \in [1, 4]$. The I_{sc} at non-standard condition is given by Eq. (17):

$$I_{sc}(G, T) = I_{sc-STC}\frac{G}{G_{STC}} + \alpha(T - T_{STC}) \quad (17)$$

where G and T stand for the temperature and the irradiation levels, respectively. The optimal estimated parameters for both SDM and DDM, of the three PV modules, at different levels of irradiation and a constant value of temperature, are provided in Tables 7 and 8, respectively. To verify the accuracy of the extracted optimal parameters of the PV model, the estimated electric current is calculated and the (I-V) characteristics of the three different modules are plotted at different irradiation levels as depicted in Figs. 7–9.

In addition, the extracted parameters of the three types of PV modules, at different values of temperature and constant level of irradiation, are given in Tables 9–11. The experimental and the estimated (I-V) characteristics are compared as shown in Figs. 10–12. Regarding the SDM, it can be seen that, for the three PV modules, the (I-V) curves obtained from the extracted optimal parameters are very close to the measured curves, under different temperatures and irradiation levels. From Table 9, a low RMSE value is obtained. Particularly, at low irradiation level, the accuracy of the estimated SDM is proven. In fact, in these circumstances, the module is subjected to certain mismatch conditions such as partial shading. Moreover, the optimal extracted results agree with FPA [15] and BFA [37]. It is verified that the series resistant R_s for the Thin-film module is around 1 and less than 0.4 for Multi-crystalline and Mono-crystalline. Concerning the DDM, it can be found that, under all different environmental conditions, the estimated results strongly fit the experimental data, even under low irradiation levels, and ensure a low RMSE value. Moreover, the value of the series resistance R_s falls within the interval [1.1, 1.147] for Thin-film ST40, and is around 0.3 for Multi-crystalline and Mono-crystalline which agree with the results in [15].

The MPP data between the MPSO algorithm and data sheet under STC ($G = 1000$ W/m^2 and $T = 25$ °C)) are compared in Table 12. From the tabulated values, it is inferred that the error between the power at MPP obtained from the estimated model and the power at MPP provided by the data sheet is less than 1% for the three types of modules.

7. Conclusion

In this research paper, an improved mutated PSO algorithm has been proposed for solar cell and module parameter extraction. In order to ameliorate the exploration process and avoid the premature convergence, the mutation concept is included in the PSO by means of an adaptive mutation probability. The MPSO ensures a trade-off among the exploration and exploitation process. To evaluate the proposed algorithm, measured data from the literature, experimental data from the laboratory work and data from the manufacturer's data sheet are used at different irradiation levels and temperature values. The validation of the results is attained through a comparative study with other optimisation techniques. The proposed algorithm provides accurate results and achieves the best RMSE values. Consequently, it can be drawn that the proposed algorithm is a good candidate for PV solar cell and module parameter extraction.

Appendix A. Supplementary material

Supplementary data associated with this article can be found, in the online version, at https://doi.org/10.1016/j.enconman.2018.08.081.

References

[1] Kermadi M, Berkouk EM. Artificial intelligence-based maximum power point tracking controllers for photovoltaic systems: comparative study. Renew Sustain Energy Rev 2017;69:369–86. https://doi.org/10.1016/j.rser.2016.11.125http://www.sciencedirect.com/science/article/pii/S1364032116308759.

[2] Bi Ziqiang, Ting Tiew On, Hao Shiyuan, Hao Wanjun. Comparative performance on photovoltaic model parameter identification via bio-inspired algorithms. Sol Energy 2016;132:606–16. https://doi.org/10.1016/j.solener.2016.03.033.

[3] XiaofangYuan, Xiang Yongzhong, He Yuqing. Parameter extraction of solar cell models using mutative-scale parallel chaos optimization algorithm. Sol Energy 2014;108:238–51. https://doi.org/10.1016/j.solener.2014.07.013.

[4] de Blas MA, Torres JL, Prieto E, Garca A. Selecting a suitable model for characterizing photovoltaic devices. Renew Energy 2002;25:371–80.

[5] Celik Ali Naci, Acikgoz Nasir. Modelling and experimental verification of the operating current of mono-crystalline photovoltaic modules using four- and five-parameter models. Appl Energy 2007;84(1):1–15. https://doi.org/10.1016/j.apenergy.2006.04.007.

[6] Easwarakhanthan T, Bottin J, Bouhouch I, Boutrit C. Nonlinear minimization algorithm for determining the solar cell parameters with microcomputers. Int J Sol Energy 1986;4(1):1–12. https://doi.org/10.1080/01425918608909835.

[7] Gottschalg R, Rommel M, Infield DG, Kearney MJ. The influence of the measurement environment on the accuracy of the extraction of the physical parameters of solar cells. Meas Sci Technol 1999;10:796.

[8] Ismail MS, Moghavvemi M, Mahlia TMI. Characterization of pv panel and global optimization of its model parameters using genetic algorithm. Energy Convers Manage 2013;73:10–25. https://doi.org/10.1016/j.enconman.2013.03.033.

[9] AlHajri MF, El-Naggar KM, AlRashidi MR, Al-Othman AK. Optimal extraction of solar cell parameters using pattern search. Renew Energy 2012;44:238–45. https://doi.org/10.1016/j.renene.2012.01.082.

[10] El-Naggar KM, AlRashidi MR, AlHajri MF, Al-Othman AK. Simulated annealing algorithm for photovoltaic parameters identification. Sol Energy 2012;86(1):266–74. https://doi.org/10.1016/j.solener.2011.09.032.

[11] Askarzadeh Alireza, Rezazadeh Alireza. Extraction of maximum power point in solar cells using bird mating optimizer-based parameters identification approach. Sol Energy 2013;90:123–33. https://doi.org/10.1016/j.solener.2013.01.010.

[12] Askarzadeh Alireza, Rezazadeh Alireza. Artificial bee swarm optimization algorithm for parameters identification of solar cell models. Appl Energy 2013;102:943–9. https://doi.org/10.1016/j.apenergy.2012.09.052.

[13] Macabebe EQB, Sheppard CJ, van Dyk EE. Parameter extraction from IV characteristics of PV devices. Sol Energy 85(1). https://doi.org/10.1016/j.solener.2010.11.005. URL http://www.sciencedirect.com/science/article/pii/S0038092X10003452.

[14] Gaing Z-L. A particle swarm optimization approach for optimum design of pid controller in avr system. IEEE Trans Energy Convers 2004;19(2):384–91. https://doi.org/10.1109/TEC.2003.821821.

[15] Alam DF, Yousri DA, Eteiba MB. Flower pollination algorithm based solar pv parameter estimation. Energy Convers Manage 2015;101:410–22. https://doi.org/10.1016/j.enconman.2015.05.074.

[16] Ram JP, Babu TS, Dragicevic T, Rajasekar N. A new hybrid bee pollinator flower pollination algorithm for solar PV parameter estimation. Energy Convers Manage 2017;135:463–76. https://doi.org/10.1016/j.enconman.2016.12.082http://www.sciencedirect.com/science/article/pii/S0196890416311773.

[17] Xu Shuhui, Wang Yong. Parameter estimation of photovoltaic modules using a hybrid flower pollination algorithm. Energy Convers Manage 2017;144:53–68. https://doi.org/10.1016/j.enconman.2017.04.042.

[18] Chellaswamy C, Ramesh R. Parameter extraction of solar cell models based on adaptive differential evolution algorithm. Renew Energy 2016;97:823–37. https://doi.org/10.1016/j.renene.2016.06.024.

[19] Awadallah MA. Variations of the bacterial foraging algorithm for the extraction of PV module parameters from nameplate data. Energy Convers Manage 2016;113:312–20. https://doi.org/10.1016/j.enconman.2016.01.071<http://www.sciencedirect.com/science/article/pii/S019689041630019X>.

[20] Yu K, Liang JJ, Qu BY, Chen X, Wang H. Parameters identification of photovoltaic models using an improved JAYA optimization algorithm. Energy Convers Manage 2017;150:742–53. https://doi.org/10.1016/j.enconman.2017.08.063<http://www.sciencedirect.com/science/article/pii/S0196890417307847>.

[21] Fathy A, Rezk H. Parameter estimation of photovoltaic system using imperialist competitive algorithm. Renew Energy 2017;111:307–20. https://doi.org/10.1016/j.renene.2017.04.014<http://linkinghub.elsevier.com/retrieve/pii/S0960148117303191>.

[22] Ye Meiying, Wang Xiaodong, Xu Yousheng. Parameter extraction of solar cells using particle swarm optimization. J Appl Phys 105(9). https://doi.org/10.1063/1.3122082.

[23] Khanna V, Das BK, Bisht D, Vandana, Singh PK. A three diode model for industrial solar cells and estimation of solar cell parameters using PSO algorithm. Renew Energy 2015;78:105–13. https://doi.org/10.1016/j.renene.2014.12.072<http://www.sciencedirect.com/science/article/pii/S0960148115000063>.

[24] Sandrolini L, Artioli M, Reggiani U. Numerical method for the extraction of photovoltaic module double-diode model parameters through cluster analysis. Appl Energy 2010;87(2):442–51.

[25] Ye M, Zeng S, Xu Y. An extraction method of solar cell parameters with improved particle swarm optimization. ECS Trans 2010;27(1):1099–104. https://doi.org/10.1149/1.3360756<http://ecst.ecsdl.org/content/27/1/1099>.

[26] J.C.X.L.S.D. Huang, W., Extracting solar cell model parameters based on chaos

particle swarm algorithm, 2011, pp. 398–402. https://doi.org/10.1109/ICEICE.2011.5777246.
[27] Jordehi A. Time varying acceleration coefficients particle swarm optimisation (tvacpso): a new optimisation algorithm for estimating parameters of pv cells and modules. Energy Convers Manage 2016;129:262–74. https://doi.org/10.1016/j.enconman.2016.09.085.
[28] Bana S, Saini RP. Identification of unknown parameters of a single diode photovoltaic model using particle swarm optimization with binary constraints. Renew Energy 101. https://doi.org/10.1016/j.renene.2016.10.010. URL http://www.sciencedirect.com/science/article/pii/S0960148116308746.
[29] Shockley W. The theory of p-n junctions in semiconductors and p-n junction transistors. Bell Syst Tech J 1949;28(3):435–89. https://doi.org/10.1002/j.1538-7305.1949.tb03645.x.
[30] Oliva D, Cuevas E, Pajares G. Parameter identification of solar cells using artificial bee colony optimization. Energy 2014;72:93–102. https://doi.org/10.1016/j.energy.2014.05.011<http://www.sciencedirect.com/science/article/pii/S036054421400560X>.
[31] Ishaque K, Salam Z, Shamsudin A, Amjad M. A direct control based maximum power point tracking method for photovoltaic system under partial shading conditions using particle swarm optimization algorithm. Appl Energy 2012;99:414–22. https://doi.org/10.1016/j.apenergy.2012.05.026<http://www.sciencedirect.com/science/article/pii/S0306261912003996>.
[32] Alrashidi MR, El-Naggar Khaled M, AlHajri MF. A new estimation approach for determining the i-v characteristics of solar cells. Sol Energy 2011;85(7):1543–50. https://doi.org/10.1016/j.solener.2011.04.013.
[33] Ifri-250-60 poly-crystalline pv module. URL <https://akafi.net/storage/upload/1179625_1408966265.pdf>.
[34] Shell sm55 photovoltaic solar module. URL <http://www.aeet-service.com/pdf/shell/Shell-Solar_SM55.pdf>.
[35] Kc200gt,high efficiency multicrystal photovoltaic module. URL <https://www.kyocerasolar.com/dealers/product-center/archives/spec-sheets/KC200GT.pdf>.
[36] Shell st40 photovoltaic solar module. URL <http://www.aeet-service.com/pdf/shell/Shell-Solar_ST40.pdf>.
[37] Rajasekar N, Kumar Neeraja Krishna, Venugopalan Rini. Bacterial foraging algorithm based solar pv parameter estimation. Sol Energy 2013;97:255–65. https://doi.org/10.1016/j.solener.2013.08.019.